ISSN 0020-1685, Inorganic Materials, 2016, Vol. 52, No. 6, pp. 604–610. © Pleiades Publishing, Ltd., 2016.
Original Russian Text © A.M. Kut'in, A.D. Plekhovich, V.V. Dorofeev, 2016, published in Neorganicheskie Materialy, 2016, Vol. 52, No. 6, pp. 656–663.

# A Mathematical Model for Analysis of Sequentially Coupled Crystallization–Melting Differential Scanning Calorimetry Peaks and the Use of the Model for Assessing the Crystallization Resistance of Tellurite Glasses

**A. M. Kut'in[a,b], A. D. Plekhovich[b], and V. V. Dorofeev[b]**

[a] *Lobachevsky State University, pr. Gagarina 23, Nizhny Novgorod, 603950 Russia*
[b] *Devyatykh Institute of Chemistry of High-Purity Substances, Russian Academy of Sciences, ul. Tropinina 49, Nizhny Novgorod, 603950 Russia*
*e-mail: plehovich@gmail.com*

Received December 4, 2015

**Abstract**—Differential scanning calorimetry (DSC) characterization of tellurite glasses doped with lanthanum oxide, which improves their crystallization resistance, has revealed a phase transformation specific to such glasses, in which partial crystallization of a sample is followed by melting of the crystals formed. The experimentally observed dependence of the decrease of crystallization–melting peaks across a series of disperse samples of $(TeO_2)_{0.72}(WO_3)_{0.24}(La_2O_3)_{0.04}$ glass with increasing particle size upon extrapolation to the size of a bulk sample has been used to assess the crystallization resistance of tellurite glasses for optical applications. The assessment technique comprises DSC characterization of particle-size-classified glass samples and the use of a mathematical model for obtaining the degree of crystallization as a function of temperature and time, $\alpha(T, t)$ through analysis of nonisothermal DSC peaks representing a partial glass crystallization process passing into melting. The crystallization resistance of glass is estimated by extrapolating the maximum $\alpha$ values as a function of particle size to a preform size. Tested for $(TeO_2)_{0.72}(WO_3)_{0.24}(La_2O_3)_{0.04}$ glass, the technique offers the possibility of selecting preforms for producing fibers from compositionally new, chemically pure tellurite glasses at a given phase purity level.

*Keywords:* crystallization resistance, tellurite glasses, mathematical model
**DOI:** 10.1134/S0020168516060066

## INTRODUCTION

In a series of tellurite glass-forming systems, which are of considerable interest as materials for fiber-optic applications and active amplification and lasing elements, tungstate–tellurite glasses offer broader Raman scattering bands and dissolve larger amounts of rare-earth oxides than do $SiO_2$-based glasses. Unfortunately, their potentialities have not yet been completely realized because of the rather high optical loss (hundreds of dB/km) in tungstate–tellurite glass fibers in the near- and mid-IR spectral regions [1–3]. The loss is due to both the presence of residual impurity phases after purification of the glasses and the formation of crystalline microinclusions, which, along with other factors, determine the phase purity of the glass.

When high-purity starting components are used, the crystallization resistance of tellurite glasses can be improved by adding, for example, 4–10 mol % lanthanum oxide. Differential scanning calorimetry (DSC) curves of massive glass samples containing $\geqslant$4 mol % $La_2O_3$ at heating rates in the range 5–10 K/min show no crystallization events (Fig. 1). Implicit peaks, attributable to crystallization with some degree of certainty, defy quantitative analysis at lower temperature scan rates. At the same time, the crystallization behavior of glasses for optical fiber fabrication is of paramount importance because, after mechanical processing, preforms have defects on their outer surface and possible surface defects on their core/cladding interface. Crystallization at such centers may increase optical losses in the fiber, especially if fiber drawing conditions have not been optimized.

The influence of surface defects on the crystallization behavior of glass can be increased and the corresponding DSC signal can be made reliably measurable by crushing bulk glass samples. Figure 2 shows DSC curves of size-classified disperse $(TeO_2)_{0.72}(WO_3)_{0.24}(La_2O_3)_{0.04}$ (TWL) glass samples, which demonstrate a tendency for crystallization processes to become less pronounced with decreasing particle size. Such a tendency is difficult to describe quantitatively, because there is no model for evaluating the degree of crystallization (volume frac-

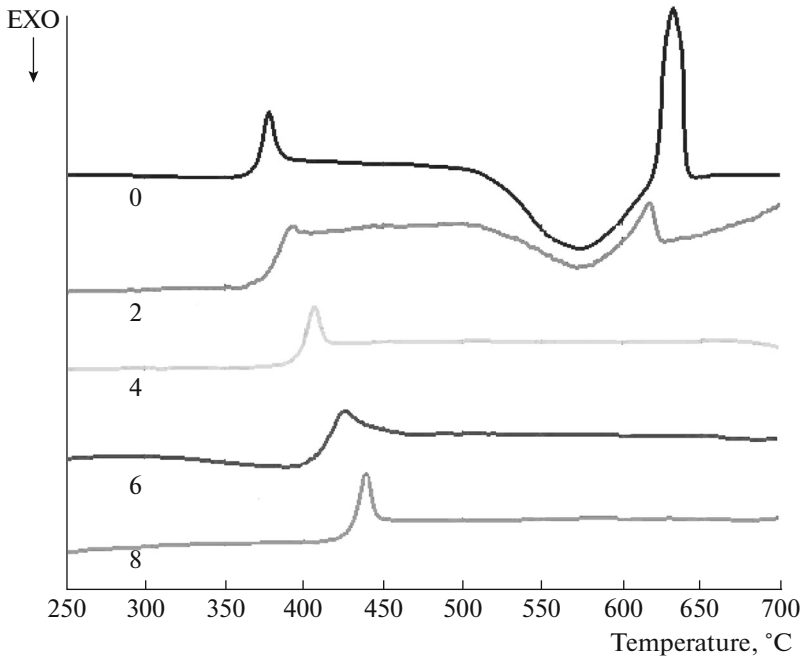


**Fig. 1.** DSC curves of $x\mathrm{TeO_2} \cdot (100 - x - z)\mathrm{WO_3} + z\mathrm{La_2O_3}$ glasses with $z$ = 0, 2, 4, 6, and 8% (compact samples in the form of disks 5 × 1.5 mm in dimensions) at a heating rate of 10 K/min.

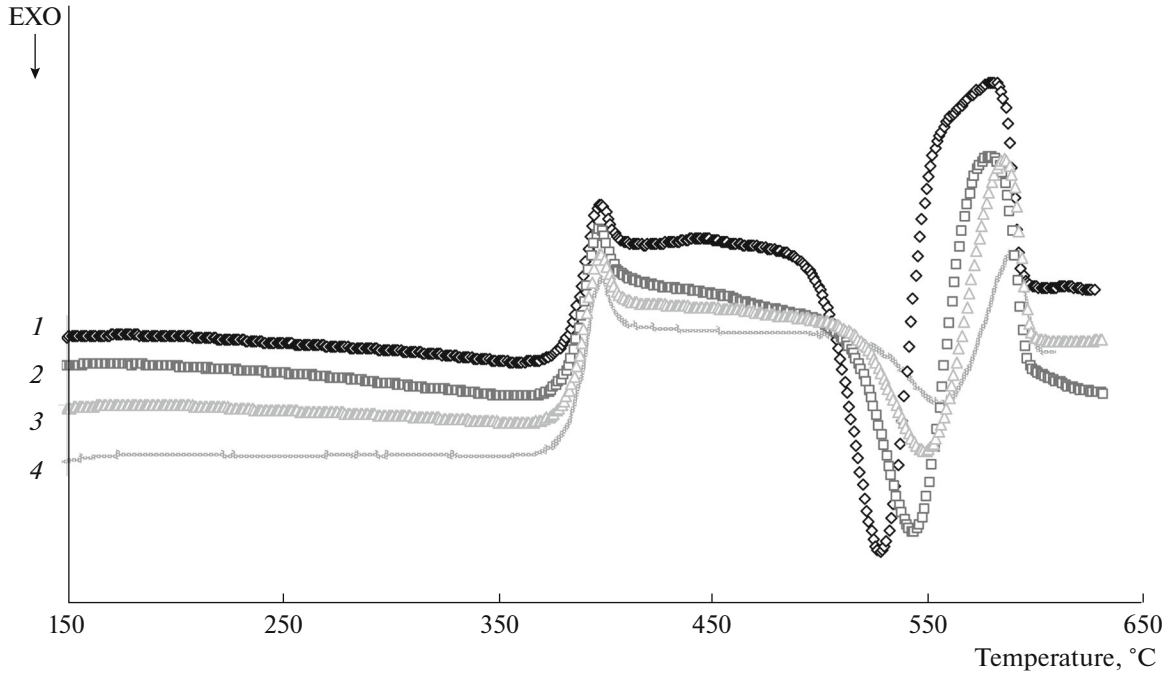


**Fig. 2.** DSC curves of size-classified TWL glasses: (*1*) 0.03–0.094, (*2*) 0.094–0.14, (*3*) 0.14–0.355, and (*4*) 0.355–0.45 mm (heating rate of 5 K/min).

tion of crystals in glass) as a function of temperature and time, $\alpha(T, t)$, for observed overlapping crystallization–melting DSC peaks.

The objectives of this work are to develop a technique for a comparative evaluation of the crystallization resistance of tellurite glasses using a mathematical model for analysis of DSC peaks of phase transformations in a number of samples differing in particle size, followed by extrapolation of the degree of crystallization to the fiber preform size, and to test the technique

with application to $(TeO_2)_{0.72}(WO_3)_{0.24}(La_2O_3)_{0.04}$ glass.

## THEORETICAL ANALYSIS

Mathematical modeling of crystallization–melting processes from DSC curves is based on a modified semiempirical (MSE) model for crystallization, whose integral form can be represented as [4]

$$\alpha = \frac{1}{(1+\tau^{-n})^p}, \quad (1)$$

where $\tau = kt$ is the product of the rate constant $k = A\exp(-E/(RT)) = \exp(s - \theta/T)$ and time $t$. The representation of the Arrhenius formula using the logarithm of the preexponential factor, $s = \ln A$, and the activation energy on the temperature scale $\theta = E/R$, is more convenient for calculations.

The corresponding differential form of the model, which defines the crystallization rate $\dot{\alpha}$, is the result of the differentiation of the degree of crystallization (1):

$$\dot{\alpha} = \frac{d\alpha}{dt} = k\alpha'_\tau = knp\alpha^{1-1/(np)}(1-\alpha^{1/p})^{1+1/n}. \quad (2)$$

First, the MSE model functionally corresponds to the semiempirical model $\dot{\alpha} = k'\alpha^q \times (1-\alpha)^r$ [5]. Second, at $p = 1$ the number and meaning of its parameters correspond to a simplified version of the well-known Kolmogorov–Johnson–Mehl crystallization model [6, 7], which characterizes the process by the activation parameters $A$ and $E$ and the power-law dimensional parameter $n$. Finally, mathematically reflecting the asymmetry of the DSC crystallization peak, the parameter $p$ extends the fitting capabilities of the MSE model to four-parameter semiempirical model.

A single, incomplete crystallization process, passing into melting, can be considered from the viewpoint of a reversible reaction underlying the A ↔ *A phase transformation of substance A from a supercooled, liquid state to a crystalline state, *A. The symbol of a crystalline state of the substance and the quantities (see below) related to this state are labeled by an asterisk in the position of a front superscript. The known expression [8] for the rate of a reversible heterogeneous reaction under diffusion control has the form

$$J = \frac{1-\exp(^*\tilde{\mu}-\tilde{\mu})}{\frac{1}{\beta_A c_A}+\frac{\exp(^*\tilde{\mu}-\tilde{\mu})}{\beta_{*A}c_{*A}}} = \frac{\exp(-(^*\tilde{\mu}-\tilde{\mu})/2)-\exp((^*\tilde{\mu}-\tilde{\mu})/2)}{\frac{\exp(-(^*\tilde{\mu}-\tilde{\mu})/2)}{\beta_A c_A}+\frac{\exp((^*\tilde{\mu}-\tilde{\mu})/2}{\beta_{*A}c_{*A}}}.$$

The second symmetrized form was obtained by multiplying the numerator and denominator by $e^{-(^*\tilde{\mu}-\tilde{\mu})/2}$. The exponent of supersaturation, equal to the difference between reduced chemical potentials (divided by $RT$), $^*\tilde{\mu}-\tilde{\mu}$, separates the reactant flow ($\beta c$) (makes it a determining factor) and reduces the importance ($\beta c$) for the reaction product, allowing the latter to admit its equality with the starting $\beta_{*A}c_{*A} = \beta_A c_A = \beta c$. Here $\beta$ is the mass transfer coefficient and $c$ is the concentration of a component of the reaction. Using the hyperbolic tangent function, we obtain

$$J = \beta c \tanh\left(-\frac{^*\tilde{\mu}-\tilde{\mu}}{2}\right).$$

In the problem under consideration, where the role of a flow quantity ($\beta c$) is played by the crystallization rate (2), the rate of the crystallization–melting process is, by analogy, supplemented by the thermodynamic factor $\tanh\left(-\frac{^*\tilde{\mu}-\tilde{\mu}}{2}\right)$:

$$\dot{\alpha} = kpn\tanh\left(-\frac{^*\tilde{\mu}-\tilde{\mu}}{2}\right)\alpha^{1-1/(np)}(1-\alpha^{1/p})^{1+1/n}. \quad (2')$$

In what follows, a necessary consistency between the differential and integral forms is ensured by the functional extension of the parameter $n$:

$$\tilde{n} = n\tanh(-\tilde{g}),\ \tilde{g} = \frac{^*\tilde{\mu}-\tilde{\mu}}{2}. \quad (3)$$

Subsequent differentiation of the integral form

$$\alpha = \frac{1}{(1+\tau^{-\tilde{n}})^p} \quad (4)$$

with respect to time, which does not influence the temperature-dependent function $\tilde{n}$, leads to an expression that formally corresponds to (2), where the parameter $n$ is replaced by $\tilde{n}$, as a result of which the rate of the crystallization–melting process contains the necessary thermodynamic factor:

$$\dot{\alpha} = k\tilde{n}p\alpha^{1-1/(\tilde{n}p)}(1-\alpha^{1/p})^{1+1/\tilde{n}}. \quad (5)$$

For the process under consideration, which takes place in a relatively narrow temperature range, where the enthalpy of the transition, $L$, can be thought to be constant, supersaturation can be expressed [9] through the temperature of the transition from crystallization to melting, $T_m$, and a dimensionless constant $\tilde{S}_m = \frac{L}{RT_m}$. Note that, for a device calibrated at a particular heating rate, the point where a DSC curve intersects the abscissa will correspond to the melting point:

$$\tilde{g} = \frac{^*\tilde{\mu}-\tilde{\mu}}{2} = \frac{1}{2}\frac{L}{RT_m}\left(1-\frac{T_m}{T}\right) = \frac{\tilde{S}_m}{2}\left(1-\frac{T_m}{T}\right). \quad (6)$$

In comparison with an isothermal version of the model, represented by expressions (3)–(6), in its nonisothermal version Eq. (5) is changed. Note that differentiating Eq. (4) with respect to time requires taking into account all quantities that depend on the sample

Parameters of the kinetic model for incomplete crystallization DSC peaks passing into melting for four size-classified $(TeO_2)_{0.72}(WO_3)_{0.24}(La_2O_3)_{0.04}$ glass samples

| Size fraction, mm | 0.03–0.094 | 0.094–0.144 | 0.144–0.355 | 0.355–0.45 |
|---|---|---|---|---|
| $n$ | 5.41 | 5.9706 | 3.8253 | 3.1384 |
| $p_0$ | 0.54898 | 0.5989 | 0.7984 | 1.2359 |
| $s_0 = \ln A$ [$s^{-1}$] | 50.974 | 50.536 | 43.974 | 38.296 |
| $\theta/T_m$ | 64.3565 | 63.57 | 58.22 | 51.00 |
| $\Delta p$ | 8.42977 | 10.035 | 12.968 | 17.93 |
| $\Delta s$ | 304.588 | 257.0 | 307.93 | 387.96 |
| $a$ | 49.543 | 47.433 | 40.104 | 29.138 |
| | 10.063 | 12.787 | 24.475 | 36.241 |
| $b$ | 1.0176 | 1.0126 | 1.0159 | 1.0219 |
| | 1.2405 | 1.1714 | 1.1031 | 1.0847 |
| $\dot{T}^*$, K/s | $8.09 \times 10^{-5}$ | $2.93 \times 10^{-4}$ | $3.85 \times 10^{-4}$ | $6.54 \times 10^{-4}$ |
| | $5.14 \times 10^{-3}$ | $3.61 \times 10^{-3}$ | $1.65 \times 10^{-3}$ | $9.68 \times 10^{-4}$ |

Normalization constants for heating rates of 2, 5, and 10 K/min are $C_N = 326.85$, 299.63, and 254.10 μV s/mg, respectively. The auxiliary parameters $a$, $b$, and $\dot{T}^*$ of function (8) in the upper lines determine the change in the main model parameter $p$ in going from crystallization to melting, and those in the lower lines determine the change of the parameter $s$ according to formulas (7).

temperature. If it is a linear function of time, $T = T_0 + \dot{T}t$, the rate of the crystallization–melting process takes the form

$$\dot{\alpha} = k\left(1 + \frac{\dot{T}t}{T}\left(\frac{k'}{k} + \frac{n''}{\tilde{n}}\ln\tau\right)\right)\tilde{n}p\alpha^{1-1/(\tilde{n}p)} \times (1-\alpha^{1/p})^{1+1/\tilde{n}} + \frac{\dot{T}\Delta p}{Tp}w_p'\alpha\ln\alpha, \quad (5')$$

where $\dot{T}$ is the temperature scan rate.

The distinction between the kinetics of the crystallization and melting processes in the model under development is taken into account by changing its parameters after $T_m$ is reached:

$$p = p_0 + w_p\Delta p,$$
$$s - \theta/T = s_0 - \theta_0/T + w_k(\Delta s - \Delta\theta/T). \quad (7)$$

A rather sharp, but continuous change from the crystallization parameters at $w = 0$ (denoted by the subscript "0") to melting parameters ($w = 1$) is ensured by auxiliary "inclusion" functions:

$$w = 0.5(1 + \tanh X), \quad X = a(T/T_m - b - \dot{T}^*/\dot{T}). \quad (8)$$

In deriving (5'), the derivatives of these functions should also be taken into account:

$$w' = T(dw/dT) = 0.5a(T/T_m)/\cosh^2 X. \quad (9)$$

Note that, like (9), all of the primed derivatives are taken with respect to a relative temperature change:

$$\tilde{n}'/\tilde{n} = \frac{T_m\tilde{S}_m}{T\sinh(-2\tilde{g})}, \quad k'/k = \theta_0/T + w_k'\Delta s. \quad (10)$$

The change in the rate constant in (10) due to some uncertainty in the activation energy for melting is only referred to $\Delta s$; that is, $\Delta\theta = 0$.

## EXPERIMENTAL

$(TeO_2)_{0.72}(WO_3)_{0.24}(La_2O_3)_{0.04}$ glass samples were studied using conventionally calibrated DSC-404 F1 Pegasus instrument. Measurements were performed in flowing Ar (80 mL/min) at heating rates of 2, 5, and 10 K/min, using platinum crucibles, which are the least reactive with such glasses, and disk-shaped samples weighing 30 mg.

The glass was prepared using high-purity tellurium dioxide [10] and commercially available extrapure-grade tungsten and lanthanum oxides. The total content of 3$d$ transition metals in the glass-forming oxide mixture was under 1 ppm [11, 12]. The glass was prepared by the crucible melting of a glass batch in a hermetically sealed quartz glass chamber under a purified oxygen atmosphere. The bulk glass preparation process [12] included melting of a batch for several hours at 800°C, followed by melt casting into a quartz glass mold and annealing at the glass transition temperature. From the bulk glass, we prepared disks ≈5 mm in diameter and ≈2 mm in thickness by mechanical processing (cutting, grinding, and polishing). In such glass samples, containing 4–10 mol % lanthanum oxide, no crystallization was detected by DSC at a heating rate of 5 or 10 K/min (Fig. 1).

Samples with a particle size distribution in the range 30–450 μm were prepared by comminuting the glass in an agate mortar. Next, each sample was classi-

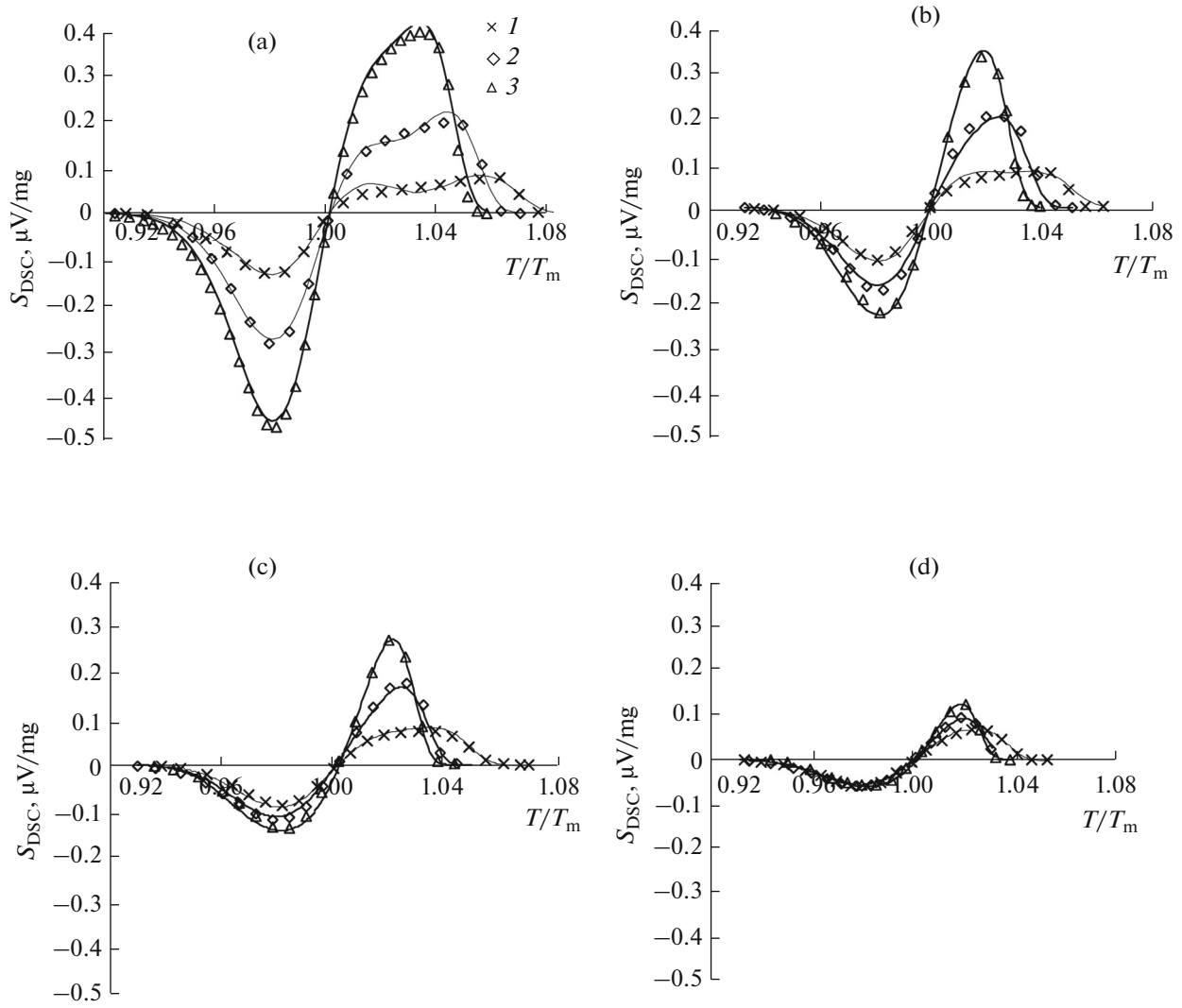


**Fig. 3.** Crystallization–melting DSC peaks of four size-classified disperse samples in the size ranges (a) 0.03–0.094, (b) 0.094–0.144, (c) 0.144–0.355, and (d) 0.355–0.45 mm at three heating rates: (*1*) 2, (*2*) 5, and (*3*) 10 K/min. The solid lines represent calculation by Eqs. (3), (4), (5'), and (6–10) with model parameters evaluated from experimental data processing results (see the table).

fied into four size ranges using sieves. The above model was used in DSC data processing for overlapping crystallization and melting peaks, which followed devitrification step in DSC curves.

## RESULTS AND DISCUSSION

The DSC signal, which is proportional to the specific heat flux $\dot{Q}_m = \frac{dQ_m}{dt} = \dot{\alpha} Q_M$ and in turn, can be expressed through the rate of the process $\dot{\alpha}$ using the specific heat of the process $Q_M$, has the form

$$S_{DSC} = C\dot{Q}_m = C\dot{\alpha}Q_M = C_N\dot{\alpha}, \qquad (11)$$

where $C_N = CQ_M$ is the instrumental or normalization constant, whose dimension is $[C_N] = [S_{DSC}/\dot{\alpha}] = \mu$Vs/mg, and $\dot{\alpha}$ is determined by formula (5') and the related equations of the model: (3), (4), and (6)–(10).

From data processing (Fig. 3, solid lines) for crystallization–melting DSC peaks (data points) by nonlinear regression, we determined model parameters (table) that quantitatively characterize the crystallization process followed by the melting of the crystallized part of the sample.

One result of practical importance is that these parameters can be used to calculate the temperature–time diagram $\alpha(T, t)$ of the process in question, which is determined by Eq. (4) and expressions (6)–(8), which appear in it. A partial case of the $\alpha(T, t)$ dependence is presented in Fig. 4 for the size fraction 0.03–0.094 mm.

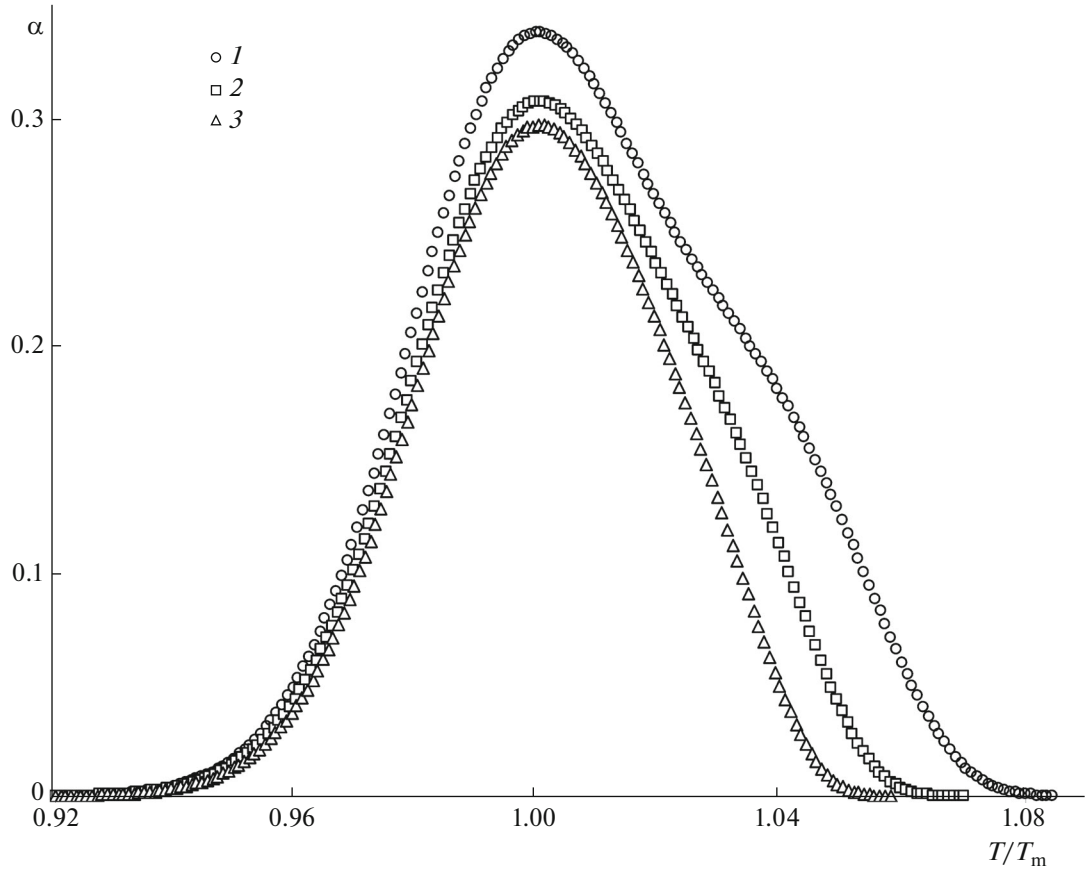


**Fig. 4.** Degree of crystallization as a function of relative temperature for a sample with particle sizes in the range 0.03–0.094 mm at heating rates of (*1*) 2, (*2*) 5, and (*3*) 10 K/min.

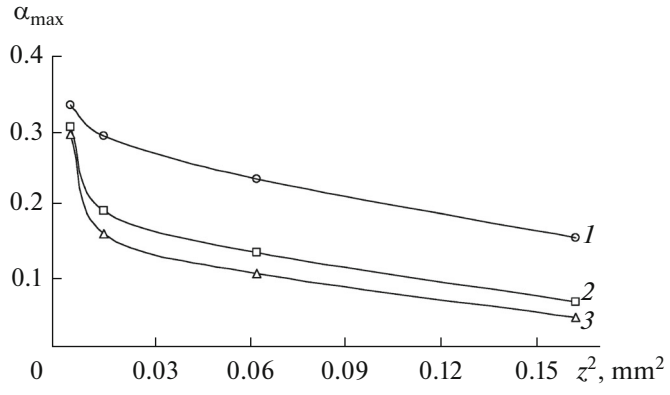


**Fig. 5.** Maximum degree of crystallization as a function of the square of the average particle size $z$ for size-classified disperse samples (data points) and theoretical fits (solid lines): $\alpha_{max} = \dfrac{L + \left(C/z^2\right)^2}{1 + \left(z^2/Z\right)^D}$ with parameters $L = 0.3064$, 0.1899, and 0.1546, $C = 7.03 \times 10^{-4}$, $1.32 \times 10^{-3}$, and $1.45 \times 10^{-3}$, $Z = 0.1634$, 0.1083, and 0.0961, and $D = 1.226$, 1.568, and 1.732, corresponding to temperature scan rates of (*1*) 2, (*2*) 5, and (*3*) 10 K/min.

The tendency for the primary crystallization–melting DSC peaks to decrease with increasing particle size in disperse samples of the glass under investigation (Fig. 3) is evidenced by the plots of the maximum degree of crystallization against average particle size in the samples in Fig. 5. The first data points in the curves in Fig. 5 correspond to the peak (maximum) values $\alpha_{max}$ in Fig. 4. Fitting functions for these dependences (see the caption to Fig. 5) allow one to make far extrapolation for estimating the degree of crystallization in a preform of finite size. For a cylindrical preform 12 mm in diameter and 60 mm in length (surface effective cube size of 20.4 mm), such an estimate at heat treatment rates of 2, 5, and 10 K/min gives $\alpha_{max} = 2.1 \times 10^{-5}$, $4.6 \times 10^{-7}$, and $7.8 \times 10^{-8}$. At an effective preform size of 30.5 mm, we obtain $\alpha_{max} = 7.6 \times 10^{-6}$, $1.3 \times 10^{-7}$, and $1.9 \times 10^{-8}$. These data confirm that the glass in question has high crystallization resistance.

## CONCLUSIONS

A mathematical analysis of DSC peaks of sequentially coupled phase transitions in tellurite glass comprises two components:

(1) a kinetic model (unavailable in the literature) for an incomplete glass crystallization process passing into melting, which allows one to extract the degree of crystallization as a function of temperature and time, $\alpha(T, t)$, from nonisothermal data, and

(2) a nonlinear regression procedure, which extrapolates the degree of crystallization to the size of a bulk sample using a number of maximum values of the degree of crystallization, $\alpha_{max}$.

Tested with application to $(TeO_2)_{0.72}(WO_3)_{0.24}(La_2O_3)_{0.04}$ tellurite glass, the technique is expected to accelerate a search for additives and choice of their optimal concentrations raising the crystallization resistance of glasses for fiber-optic applications. In particular, in the case of two glasses tested for crystallization behavior, it is sufficient to compare data processing results for four DSC curves of size-classified disperse samples for each glass obtained at a given heating rate in a narrow range of crystallization–melting temperatures.

The increasing current interest in such an independent, nonoptical test for crystallization behavior, which requires samples as small as 30 mg in weight, is aroused, in particular, by the revival—on a modern basis—of a production technology for sintering a mixture of inorganic oxide powders. A modern version of such technology, based on high-purity components, employs approaches for the fabrication of microstructured fibers [13, 14].

To characterize the proposed technique, it is reasonable to conclude that it describes crystallization primarily on already present and grinding-induced surface (heterogeneous) centers of formation of a new phase. At the same time, the semiempirical version of crystallization theory used here effectively takes into account the homogeneous component as well, without detailing its fraction. Note that the experimental DSC data processing procedure requires no information about the forming phase, nor its identification is needed.

The proposed model for analysis of crystallization–melting DSC peaks, with the possibility of determining $\alpha(T, t)$, is of interest on its own for characterization of glass-forming systems, whose characteristics are typically related to the degree of crystallinity of glass.

## ACKNOWLEDGMENTS

This work was supported by the Russian Foundation for Basic Research, grant nos. 14-03-31376 mol_a, 15-03-08324, and 15-43-02185.

## REFERENCES

1. Lin, A., Zhang, A., Bushong, E.J., and Toulouse, J., Solid-core tellurite glass fiber for infrared and nonlinear applications, *Opt. Express,* 2009, vol. 17, no. 19, pp. 16716–16721.
2. Dorofeev, V., Moiseev, A., Kraev, I., Motorin, S., Churbanov, M., Kosolapov, A., Dianov, E., Plotnichenko, V., and Philippovskiy, D., Tungstate–tellurite glass fibers for spectral region up to 3 μm, *Advanced Photonics Congress, OSA Technical Digest (Online),* Opt. Soc. of Am., 2012. doi 10.1364/ANIC.2012.JM5A.3
3. Desevedavy, S.F., Jules, J.-Ch., Gadret, G., Fatome, J., Kibler, B., Kawashima, H., Ohishi, Y., and Smektala, F., Management of OH absorption in tellurite optical fibers and related supercontinuum generation, *Opt. Mater.,* 2013, vol. 35, pp. 1595–1599.
4. Kut'in, A.M., Plekhovich, A.D., and Sibirkin, A.A., Crystallization kinetics of $(TeO_2)_{1-x}(MoO_3)_x$ glasses studied by differential scanning calorimetry, *Inorg. Mater.,* 2015, vol. 51, no. 12, pp. 1288–1294.
5. Erofeev, B.V. and Mitzkevich, N.I., *Reactivity of Solids,* Amsterdam: Elsevier, 1961, p. 273.
6. Kolmogorov, A.N., On the statistical theory of crystallization of metals, *Izv. Akad. Nauk SSSR, Ser. Mat.,* 1937, vol. 1, no. 3, pp. 355–359.
7. Johnson, W.A. and Mehl, R.F., Reaction kinetics in processes of nucleation and growth, *Trans. Am. Inst. Mineral. Eng.,* 1939, vol. 135, pp. 419–426.
8. Frank-Kamenetskii, D.A., *Diffuziya i teploperedacha v khimicheskoi kinetike* (Diffusion and Heat Transfer in Chemical Kinetics), Moscow: Nauka, 1987, p. 502.
9. Kubo, R., *Thermodynamics,* Amsterdam: North Holland, 1968. Translated under the title *Termodinamika,* Moscow: Mir, 1970, p. 304.
10. Moiseev, A.N., Chilyasov, A.V., Dorofeev, V.V., Churbanov, M.F., Snopatin, G.E., Kraev, I.A., Pimenov, V.G., and Lipatove, M.M., RF Patent 2 301 197, *Byull. Izobret.,* 2007, no. 17.
11. Dorofeev, V.V., Moiseev, A.N., Churbanov, M.F., Snopatin, G.E., Chilyasov, A.V., Kraev, I.A., Lobanov, A.S., Kotereva, T.V., Ketkova, L.A., Pushkin, A.A., Gerasimenko, V.V., Plotnichenko, V.G., Kosolapov, A.F., and Dianov, E.M., High purity $TeO_2$–$WO_3$–($La_2O_3$, $Bi_2O_3$) glasses for fiber-optics, *Opt. Mater.,* 2011, vol. 33, pp. 1911–1915.
12. Dorofeev, V.V., Moiseev, A.N., Churbanov, M.F., Kotereva, T.V., Chilyasov, A.V., Kraev, I.A., Pimenov, V.G., Ketkova, L.A., Dianov, E.M., Plotnichenko, V.G., Kosolapov, A.F., Koltashev, V.V., Production and properties of high purity $TeO_2$–$WO_3$–($La_2O_3$, $Bi_2O_3$) and $TeO_2$–ZnO–$Na_2O$–$Bi_2O_3$ glasses, *J. Non-Cryst. Solids,* 2011, vol. 357, pp. 2366–2370.
13. Velmiskin, V.V., Egorova, O.N., Mishkin, V., Nishchev, K., and Semjonov, S.L., Active material for fiber core made by powder-in-tube method: subsequent homogenization by means of stack-and-draw technique, *Proc. SPIE–Int. Soc. Opt. Eng.,* 2012, vol. 8426. doi 10.1117/12.922188
14. Bufetov, I.A., Semjonov, S.L., Vel'miskin, V.V., Firstov, S.V., Bufetova, G.A., and Dianov, E.M., Optical properties of active bismuth centres in silica fibres containing no other dopants, *Kvantovaya Elektron.* (Moscow), 2010, vol. 40, no. 7, pp. 639–641.

*Translated by O. Tsarev*